

BRAF Inhibitors Based on an Imidazo[4,5]pyridin-2-one Scaffold and a Meta Substituted Middle Ring

Arnaud Nourry,[†] Alfonso Zambon,[†] Lawrence Davies,[†] Ion Niculescu-Duvaz,[†] Harmen P. Dijkstra,[†] Delphine Ménard,[†] Catherine Gaulon,[†] Dan Niculescu-Duvaz,[†] Bart M. J. M. Suijkerbuijk,[†] Frank Friedlos,[†] Helen A. Manne,[†] Ruth Kirk,[‡] Steven Whittaker,[‡] Richard Marais,[‡] and Caroline J. Springer^{*†}

[†]*Cancer Research UK Centre of Cancer Therapeutics, The Institute of Cancer Research, 15 Cotswold Road, Sutton, Surrey SM2 5NG, United Kingdom, and* [‡]*Cancer Research UK Centre for Cell and Molecular Biology, The Institute of Cancer Research, 237 Fulham Road, London SW3 6JB, United Kingdom*

Received October 11, 2009

We recently reported on the development of a novel series of BRAF inhibitors based on a tripartite A–B–C system characterized by a para-substituted central aromatic core connected to an imidazo[4,5]pyridin-2-one scaffold and a substituted urea linker. Here, we present a new series of BRAF inhibitors in which the central phenyl ring connects to the hinge binder and substrate pocket of BRAF with a meta-substitution pattern. The optimization of this new scaffold led to the development of low-nanomolar inhibitors that permits the use of a wider range of linkers and terminal C rings while enhancing the selectivity for the BRAF enzyme in comparison to the para series.

Introduction

BRAF^a is a serine/threonine specific protein kinase and a component of the ERK MAPK cell signaling pathway that regulates essential cell responses to environmental changes.^{1,2} BRAF is also a human oncogene that is mutated in approximately 50% of malignant melanomas and at a lower frequency in a variety of other human cancers (e.g., colorectal, ovarian, and papillary thyroid cancers).^{2–5} The most common BRAF mutation in human cancer is the substitution of a valine for glutamic acid at position 600 (termed ^{V600E}BRAF), resulting in a protein that has 500-fold elevated protein kinase activity compared to the wild type. ^{V600E}BRAF stimulates sustained and constitutive activation of the ERK pathway, inducing uncontrolled cell proliferation, increased cell survival, and tumor progression.^{3,6} These data indicate that ^{V600E}BRAF is an important therapeutic target in human cancer,^{4,7,8} and some drug discovery and drug development programs have been initiated.⁹ Important advances have been made over the past decade in the field of the small molecule kinase inhibitors, with some representative marketed examples of this class of inhibitors being gefitinib¹⁰ **1**, sorafenib¹¹ **2**, and imatinib¹² **3**, shown in Figure 1.

Recently, we reported on the development of a series of type II inhibitors¹³ (Figure 2) targeting the inactive conformation of ^{V600E}BRAF for the treatment of mutant BRAF-driven malignancies.^{14,15} These compounds are based on a 2,3-dihydroimidazo[4,5]pyridin-2-one scaffold binding to the hinge region of BRAF, an aromatic system occupying the

lipophilic DFG-out pocket (BPII using the general kinase nomenclature of the kinase binding pockets),¹⁶ a linker (urea, amide, or sulfonamide) interacting with the salt bridge, and a terminal aromatic group (phenyl or pyrazole) filling the allosteric pockets created by the displacement of the DFG loop (BPIII and BPIV).^{14,15} For clarity, we have named the hinge binder, the middle ring, and the terminal aromatic group rings A, B, and C, respectively, and the salt bridge binder BC linker. This series of para-substituted compounds has shown excellent activity against the ^{V600E}BRAF enzyme, with IC₅₀ down to 1 nM and submicromolar cellular activities.¹⁵

All of the type II inhibitors that we reported on previously feature a 1,4 (para) substituted aromatic B ring connecting the hinge binding moiety with the salt-bridge linker. Docking studies of our inhibitors into the BRAF/sorafenib cocrystal structure (PDB code UWH)⁴ indicated that inhibitors with a meta substitution pattern on this ring could indeed retain the binding affinity observed for the para-substituted compounds, while moving to a novel chemical area. We later discovered that this hypothesis was supported by the fact that the meta type I BRAF binder PLX4032¹⁷ presents a 1,3 (meta) substituted central aromatic ring.

According to the docking results, the binding mode of these meta compounds in BRAF is similar to that of sorafenib.⁴ In particular, the 2,3-dihydroimidazo[4,5]pyridin-2-one unit forms a hydrogen bond with the backbone of Cys532 of the hinge region, and three more H bonds are formed by the urea moiety of the inhibitor, two between the NH groups and the Glu501 side chain and one between the carbonyl moiety and the backbone of Asp594 of the DFG motif. The chlorotri-fluoromethyl phenyl group interacts with the BPIII and BPIV hydrophobic pockets exposed by the displacement of the DFG loop in the out conformation (Figure 3). No alternative modes of binding to the target were evidenced by the docking analysis of **12** and the other meta compounds presented in this paper.

The comparison between the docking poses of the meta compound **12** and its para analogue **12a** shown in Figure 3

*To whom correspondence should be addressed. Phone: +44 20 87224214. Fax: +44 20 8722 4046. E-mail: caroline.springer@icr.ac.uk.

^a Abbreviations: RAF, rapidly growing fibrosarcoma; BRAF, V-RAF murine sarcoma viral oncogene homologue B1; MAPK, mitogen-activated protein kinase; MEK, mitogen-activated protein kinase/extracellular regulated kinase; ERK, extracellular regulated kinase; PK, pharmacokinetics; Boc, *tert*-butoxycarbonyl; DMF, dimethylformamide; TFA, trifluoroacetic acid; THF, tetrahydrofuran; DCM, dichloromethane; SAR, structure–activity relationship.

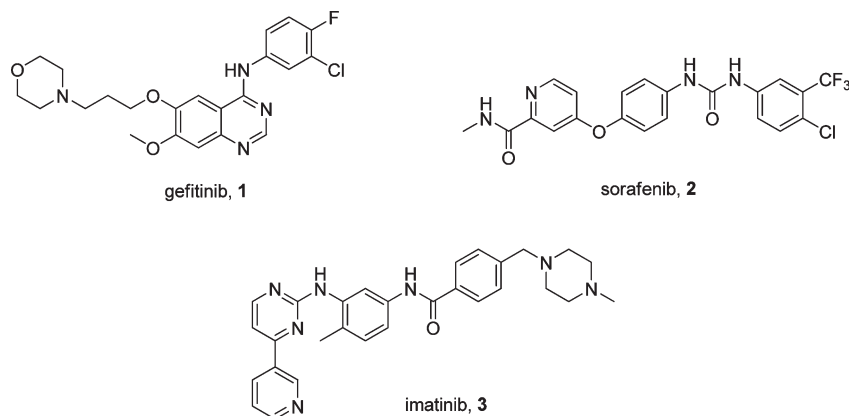


Figure 1. Structures of recent kinase inhibitors.

BPII (DFG-out pocket)

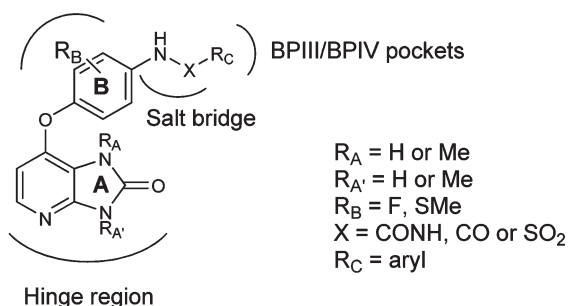


Figure 2. General structure of BRAF inhibitor series with important BRAF interactions.

suggests that the middle ring of compounds bearing a meta substitution pattern lies partially in the lipophilic BPI pocket situated next to the ATP binding site. We noticed previously¹⁵ that elaboration into the BPI pocket improved the selectivity of BRAF inhibitors toward a panel of protein kinases; one could therefore expect the meta-substituted inhibitors to present a different and improved selectivity profile with respect to the para-substituted compounds. The docking poses of the A rings of **12** and **12a** are very close, suggesting that the SAR of this moiety reported for the para series¹⁴ could be extended to a meta series. Conversely, a difference between the SAR behavior of the meta and para series could be expected for the rest of the scaffold, as the poses of the B ring–linker–C ring systems are less close (Figure 3). This prompted us to focus our medicinal chemistry efforts toward the modification of the B and C rings and of the linker, using the 2,3-dihydroimidazo[4,5]pyridin-2-one moiety as the hinge binder.

The change in the substitution pattern of the middle ring from 1,4 to 1,3 should also modify the overall conformation of the scaffold so that changes in the physicochemical properties of the compounds would be expected. The present work reports the synthesis of a variety of such inhibitors and their SAR analysis. The target scaffold for this study consists of the 2,3-dihydroimidazo[4,5]pyridin-2-one hinge binding moiety and a central phenyl ring attached in the 3-position to the terminal C ring via various linkers (Figure 4).

Chemistry

The general synthetic routes to the target compounds are depicted in Scheme 1. The first step is an aromatic nucleophilic

substitution between the 4-chloro-2-amino-3-nitropyridine and various substituted aminophenols, in which the amino group is either protected with a Boc group (**4a–c**) or unprotected (**4d–l**). The protected intermediates **5a–c** were used to access the target compounds by route A. This route consists of the formation of the AB ring system prior to the introduction of the BC linker bearing a variety of C rings and allows ready access to a panel of compounds with different BC linkers and C rings. After reduction of the nitro group of compounds **5a–c** by catalytic hydrogenation, the cyclic urea (compounds **7a–c**) was formed using triphosgene in basic conditions. Various BC linkers were then introduced from the deprotected amino group of compounds **8a–c**. The urea linker was obtained by reaction of the amine with either an isocyanate group or an activated carbamate, whereas the sulfonamide linker was introduced by reaction with an aromatic sulfonyl chloride. For the amide linker, acid chlorides or activated carboxylic acids were used as C ring precursors depending on the commercial availability of the starting material. The reduced amide linker, with a methylene bridge instead of the carbonyl group, was prepared using the corresponding substituted benzaldehyde as the C ring precursor under reductive amination conditions. The alternative route B to the target compounds was used when route A failed. In this case, the BC linker was introduced on the amino intermediates **9d–l** prior to the formation of the A ring using the same methodologies exemplified in route A.

For the synthesis of the targets **82–89** bearing a reversed amide linker (i.e., with the carbonyl group bound to the middle ring), a slightly different strategy was applied (Scheme 2), using methyl 3-hydroxybenzoate as starting material. The AB ring system was then prepared using the same methods described above, and the coupling of the linker was carried out using substituted aromatic amine in the presence of either trimethylaluminum (AlMe_3)¹⁸ or sodium bis(trimethylsilyl)amide (NaHMDS).¹⁹

Results and Discussion

The biological activities of our target compounds were evaluated using three assays as previously reported.^{14,15} The first measures the potency against the $\text{V}^{600\text{E}}$ BRAF mutant enzyme in vitro (IC_{50} , BRAF). In order to assess the inhibition of the target signaling pathway (RAF-ERK), the phosphorylation of extracellular signal-regulated kinase (ERK) was assessed in a cell-based assay (IC_{50} , pERK). Finally, the antiproliferative activity of the compounds was assessed using a sulforhodamine B (SRB) cell

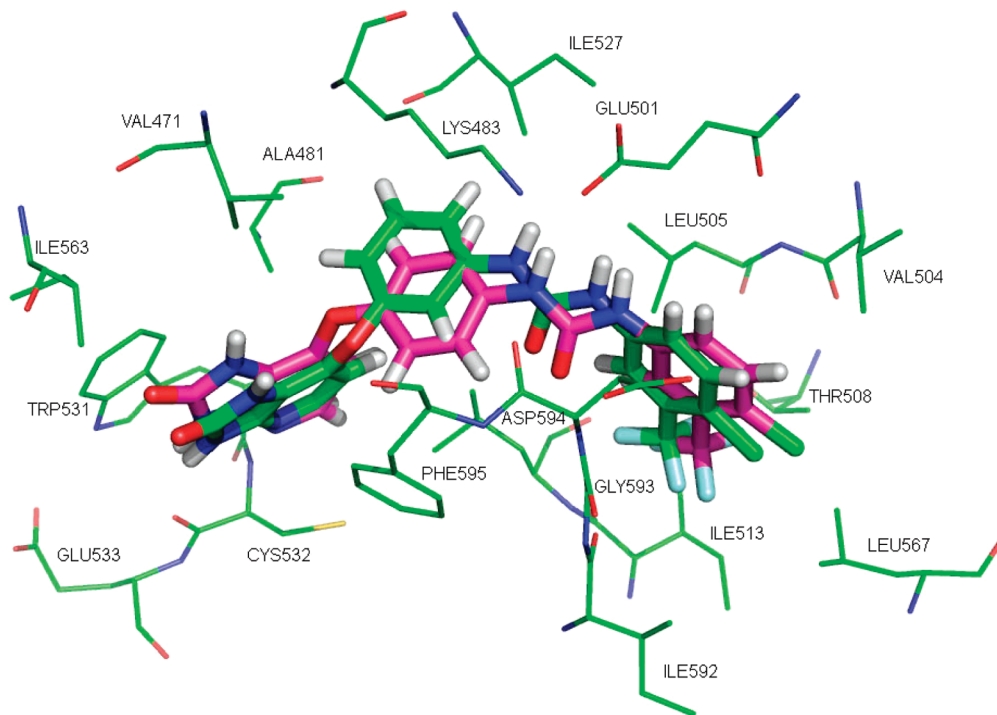


Figure 3. Superposed docking poses of meta compound **12** (green) and para **12a** (purple) in the BRAF active site.

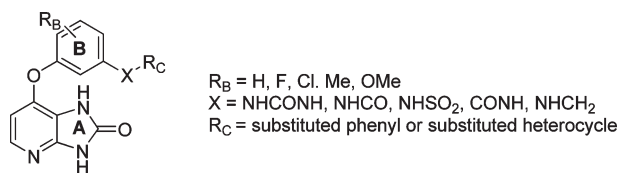


Figure 4. General structure of target series, presenting a meta substitution pattern on B ring.

proliferation assay (GI_{50} , SRB). All results are summarized in Tables 1–3.

1,3-Substitution (Meta) versus 1,4-Substitution (Para). To evaluate the effect on activity of the change in substitution pattern, we compared selected 1,3-substituted inhibitors with their corresponding 1,4- analogues, previously described.^{14,15} Table 1 shows the results obtained in the V^{600E} BRAF kinase assay for both series. In order to confirm the validity of our model, we compared the para compound **12a**,¹⁴ bearing a urea BC linker and a phenyl middle ring, with its meta counterpart **12**: the two inhibitors are essentially equipotent against V^{600E} BRAF.

We extended the comparison between the two series to other BC linker/C ring combinations. For sulfonamide linkers, all the compounds assessed (**13**–**16**) in the 1,3-series show micromolar activity against V^{600E} BRAF, whereas the corresponding analogues bearing substituted C phenyl ring in the 1,4-series (**13a**–**15a**) were inactive. Only unsubstituted **16a** has shown activity against V^{600E} BRAF (0.85 μM) and is more active than its 1,3 equivalent. The same trend was observed for the amide derivatives (**17**–**20**). For all the compounds assessed, the amides of the 1,3-series show a significant improvement in activity compared to their 1,4-series counterparts. The example with the greatest differential is compound **20**, which demonstrates a 1000-fold increase in potency with respect to its analogue **20a**.

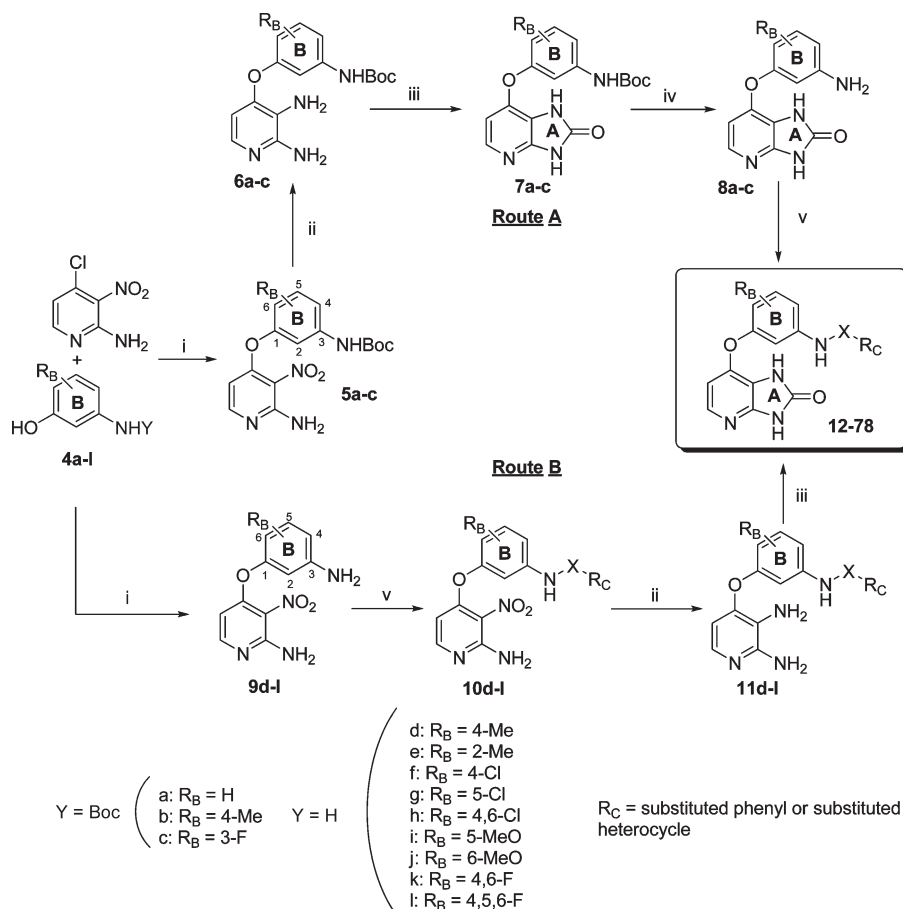
Variation of the BC Linker and the C Ring. We followed up these positive results by examining a larger panel of BC

linkers and C rings to improve in vitro potency. The biological results in the three assays (IC_{50} BRAF, IC_{50} pERK, GI_{50} SRB) are shown in Table 2.

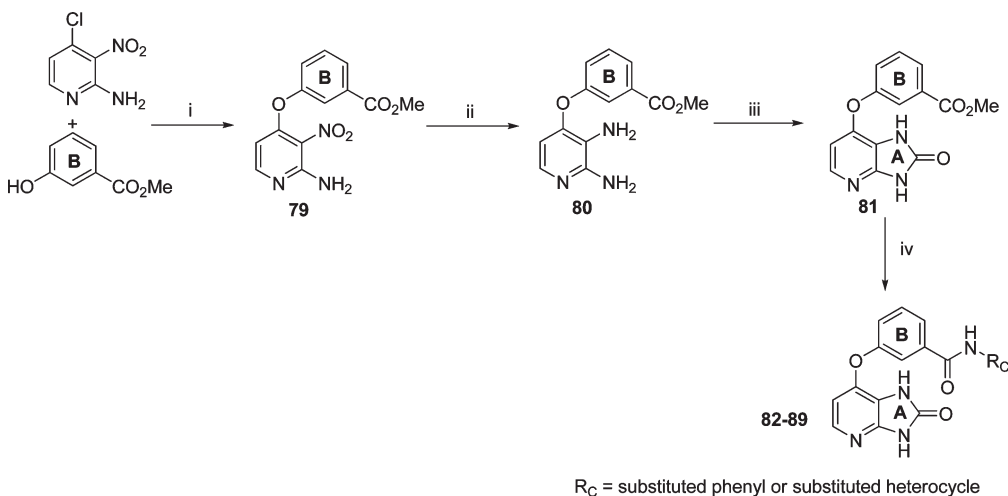
Among the compounds bearing a urea BC linker, **12** (with a 4-chloro-3-trifluoromethylphenyl C-ring) and **23** (2-fluoro-5-trifluoromethylphenyl C-ring) show good activity against V^{600E} BRAF ($IC_{50} = 15$ and 26 nM, respectively) but poor cellular activities. In the sulfonamide series, compounds **13**–**16** and **30** show poor activity in the BRAF and pERK assays.

We previously reported how the introduction of large lipophilic substituents on the middle B ring led to submicromolar cellular activities in the para series.¹⁵ Interestingly, in the meta series we observe a similar level of cellular inhibition with compounds **26**–**29**, bearing an unsubstituted middle ring in combination with 1-aryl-3-*tert*-butylpyrazoles based C rings. Compound **26** is the most effective, with a pERK IC_{50} of 830 nM and an SRB GI_{50} of 705 nM. The substitution of the *tert*-butyl group by the less bulky trifluoromethyl group in position 3 of the pyrazole (**29** versus **26**) has a negative impact on activity.

We investigated the effect of different C-rings in combination with the amide linker. Among the panel of phenyl rings explored, those bearing a fluorinated ether in the 3 position (OCF₃ or OCF₂CF₂H) are very potent against isolated V^{600E} BRAF but less active in the cellular pERK and SRB assays (**39**, **43**, **46**). The 3-trifluoromethylthiophenyl and 3-*tert*-butylphenyl groups also are favorable ($IC_{50}^{V^{600E}}$ BRAF for **47** and **48** is 5 and 17 nM, respectively). Substitution on the meta position of C ring appears essential to maintain activity (compare **39** versus **41**), and the introduction of a further methylene group between the amide linker and the phenyl ring leads to inactive compounds (compare **40** versus **39** and **35**, **36** versus **19**). The introduction of bulky groups (in **50**–**53**, **20**) or a fused ring (in **54**–**58**) on position 3 of the C ring does not lead to potency improvement in the three assays. We also explored a variety

Scheme 1. Synthesis of 1,3-Substituted Inhibitors 12–78^a

^a Reagents and conditions: (i) ^tBuOK, DMF, 80 °C; (ii) H₂, Pd/C, EtOAc/EtOH; (iii) triphosgene, THF/pyridine; (iv) TFA, room temp. (v) For X = CONH (urea): R_C isocyanate, THF, room temp or R_C carbamate, DMSO, 85 °C. For X = SO₂ (sulfonamide): R_C-sulfonyl chloride, pyridine, room temp. For X = CO (amide): R_C acid chloride, Et₃N, THF, reflux or R_C-carboxylic acid, DIC, HOBt, room temp. For X = CH₂ (reduced amide) R_C-CHO, EtOH, Na(AcO)₃BH, room temp.

Scheme 2. Synthesis of Inhibitors 82–89 with Reversed Amide BC Linker^a

^a Reagents and conditions: (i) NaH, DMSO, 100 °C; (ii) H₂, Pd/C, EtOAc/EtOH; (iii) triphosgene, THF/pyridine, reflux; (iv) R_C-NH₂, AlMe₃, THF, reflux or R_C-NH₂, NaHMDS, THF, room temp.

of heterocycles as C ring. Substituted pyridines (**59**, **60**) or pyrazoles (**61**–**66**) show moderate or poor biological activities. Compounds **65** with 3-*tert*-butyl-1-phenyl-1*H*-pyrazole and **66** with 3-isopropyl-1-phenyl-1*H*-pyrazole as C ring, analogues of the most effective pyrazole derivatives

with a urea linker, show nanomolar IC₅₀ against purified ^{v600E}BRAF (**65** and **66** show 274 and 87 nM, respectively) but have micromolar activity in the cell-based assays (13.7 μM for both compounds in the pERK assay and 3.1 and 5.7 μM, respectively, in the SRB assay).

Table 1. ^{V600E}BRAF IC₅₀ (μM) of Phenoxy-1*H*-imidazo[4,5-*b*]pyridin-2(3*H*)-ones Meta- and Para-Substituted on the Central Phenyl Ring or B Ring^a

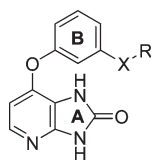
<i>Meta/Para</i>	R	IC ₅₀ ^{V600E} BRAF (μM)	
		1,3-substitution (<i>meta</i>)	1,4-substitution (<i>para</i>)*
12 / 12a		0.015	0.023
13 / 13a		6.8	> 100
14 / 14a		15.4	> 100
15 / 15a		11.3	> 100
16 / 16a		8.3	0.85
17 / 17a		0.124	15.9
18 / 18a		1.56	14
19 / 19a		25.2	> 100
20 / 20a		0.062	> 100

^a(*) a denotes para counterparts taken from refs 14 and 15 for comparison.

We investigated the effect on activity of reversing the amide moiety. The compounds substituted by a fluorinated ether group (OCF₃ or OCF₂CF₂H) or a fluorinated thioether group (SCF₃) in position 3 of the C ring show generally similar or slightly weaker biological activities (**82**, **85**, **86**). Conversely, compound **87** with 3-*tert*-butyl-1-phenyl-1*H*-pyrazole as C ring shows a significant improvement in the cell-based assays while maintaining its activity against purified ^{V600E}BRAF (**87** and **65**: 356 and 274 nM, respectively,

for ^{V600E}BRAF assay; 1.09 and 13.7 μM for pERK assay; and 0.989 and 3.1 μM for SRB assay). We also prepared an analogue of **39** in which the carbonyl group of the amide linker was removed (**67**). Unsurprisingly, removal of one of the salt-bridge binders is detrimental to ^{V600E}BRAF and pERK activity.

The choice of the most effective BC linker for the 1,3-series appears to be dependent on the C-ring used. For example, when the C-ring is the 4-chloro-3-(trifluoromethyl)phenyl

Table 2. Exploration of Various C Ring and B-C Linker Combinations

Compound	R	IC ₅₀ BRAF (μM) ± SEM	IC ₅₀ pERK (μM) ± SEM	GI ₅₀ SRB (μM) (95% CI)
Urea: X = NHCONH				
12		0.015 ± 0.004	10.7 ± 0.7	4.20 (4.11 - 4.38)
21		2.75 ± 0.36	50.2 ± 0.7	3.30 (3.07 - 3.48)
22		1.12 ± 0.09	39.0 ± 13.9	3.70 (3.46 - 3.88)
23		0.026 ± 0.002	12.2 ± 1.1	1.60 (1.48 - 1.62)
24		0.195 ± 0.003	10.3 ± 1.4	12.9 (12.6 - 14.0)
25		0.740 ± 0.280	42.0 ± 13.9	16.7 (14.9 - 18.7)
26		0.128 ± 0.013	0.830 ± 0.180	0.705 (0.682 - 0.728)
27		0.089 ± 0.005	1.33 ± 0.13	1.00 (0.97 - 1.09)
28		0.123 ± 0.022	1.96 ± 0.10	1.90 (1.75 - 2.05)
29		0.40 ± 0.12	4.80 ± 0.62	4.28 (3.98 - 4.60)
Sulfonamide: X = NHSO ₂				
13		6.80 ± 3.01	66	40.0 (39.2 - 41.2)
14		15.4 ± 4.7	57.0 ± 24.7	0.830 (0.758 - 0.901)
15		11.3 ± 1.6	94	2.96 (2.76 - 3.18)

Table 2. Continued

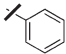
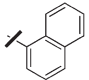
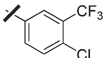
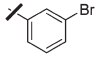
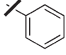
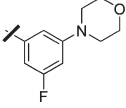
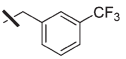
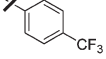
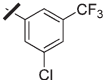
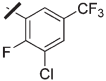
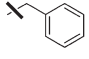
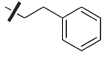
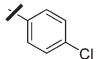
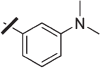
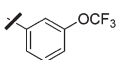
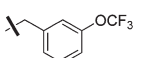
Compound	R	IC ₅₀ BRAF (μM) ± SEM	IC ₅₀ pERK (μM) ± SEM	GI ₅₀ SRB (μM) (95% CI)
Sulfonamide: X = NHSO ₂				
16		8.30 ± 1.66	29.6 ± 9.4	0.175 (0.162 - 0.190)
30		25.0 ± 1.9	21.3 ± 0.9	0.850 (0.783 - 0.915)
Amide: X = NHCO				
17		0.124 ± 0.010	28	13.4 (12.9 - 14.0)
18		1.56 ± 0.60	100	0.907 (0.830 - 0.992)
19		25.2 ± 11.5	> 100	1.54 (1.42 - 1.68)
20		0.062 ± 0.009	21.1	25.1 (23.9 - 26.3)
31		> 10	17.8 ± 2.9	25.7 (24.5 - 26.9)
32		0.730 ± 0.108	> 100	n.d
33		0.690 ± 0.113	23.9 ± 1.0	3.30 (2.94 - 3.62)
34		0.62 ± 0.20	65.0 ± 4.7	4.80 (4.26 - 5.38)
35		87	> 100	25.6 (23.7 - 28.0)
36		94	> 100	30.9 (27.3 - 35.0)
37		68	> 100	9.10 (7.35 - 11.31)
38		> 100	42	7.00 (5.93 - 8.34)
39		0.014 ± 0.001	7.56 ± 4.94	1.00 (0.92 - 1.09)
40		> 10	12.8	29.4 (26.4 - 32.8)

Table 2. Continued

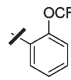
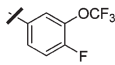
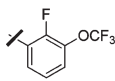
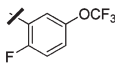
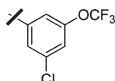
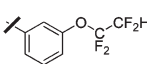
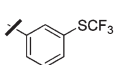
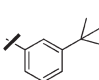
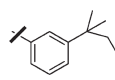
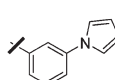
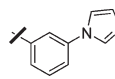
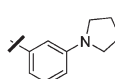
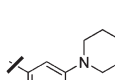
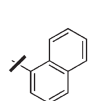
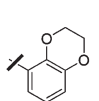
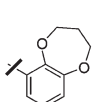
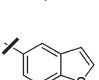
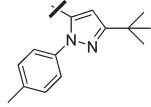
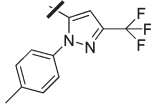
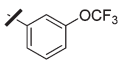
Compound	R	IC ₅₀ BRAF (μM) ± SEM	IC ₅₀ pERK (μM) ± SEM	GI ₅₀ SRB (μM) (95% CI)
Amide: X = NHCO				
41		79	35.8 ± 3.2	1.30 (1.18 - 1.33)
42		0.049 ± 0.004	27.7 ± 1.5	7.40 (7.03 - 7.74)
43		0.015 ± 0.004	6.70 ± 2.01	0.570 (0.590 - 0.609)
44		0.043 ± 0.014	15.0 ± 5.3	1.20 (1.09 - 1.22)
45		0.071 ± 0.021	14.6 ± 2.2	6.50 (6.05 - 7.02)
46		0.023 ± 0.002	5.70 ± 0.83	0.841 (0.773 - 0.916)
47		0.005 ± 0.001	6.48 ± 0.62	5.10 (4.94 - 5.24)
48		0.017 ± 0.003	3.50 ± 1.33	1.83 (1.72 - 1.94)
49		0.040 ± 0.008	3.10 ± 0.54	4.32 (4.05 - 4.62)
50		0.057 ± 0.017	20.4 ± 3.6	1.10 (0.98 - 1.11)
51		> 10	> 100	6.20 (5.74 - 6.68)
52		0.115 ± 0.069	> 100	10.0 (9.6 - 10.4)
53		0.047 ± 0.002	15.4 ± 1.1	9.60 (9.49 - 10.40)
54		0.920 ± 0.304	29.0 ± 6.8	23.0 (22.1 - 23.4)
55		> 100	> 100	40.0 (38.4 - 41.0)
56		> 100	> 100	48.0 (46.0 - 50.2)
57		22	66	1.50 (1.31 - 1.70)

Table 2. Continued

Compound	R	IC ₅₀ BRAF (μM) ± SEM	IC ₅₀ pERK (μM) ± SEM	GI ₅₀ SRB (μM) (95% CI)
Amide: X = NHCO				
58		> 100	> 100	8.30 (6.96 - 9.79)
59		93	> 100	25.0 (19.4 - 32.2)
60		1.00 ± 0.46	38.8 ± 0.3	61.0 (49.0 - 76.4)
61		> 100	79.0 ± 18.1	15.3 (14.5 - 16.1)
62		> 100	92	15.6 (14.6 - 16.5)
63		> 100	> 100	10.5 (8.9 - 12.3)
64		> 100	38.0 ± 5.0	3.30 (2.96 - 3.75)
65		0.274 ± 0.070	13.7 ± 3.0	3.10 (2.97 - 3.26)
66		0.087 ± 0.031	13.7 ± 4.3	5.7 (5.4 - 6.0)
“Reversed amide”: X = CONH				
82		0.048 ± 0.014	14.6 ± 2.1	2.40 (2.25 - 2.50)
83		0.090 ± 0.014	8.20 ± 0.42	7.30 (6.79 - 7.85)
84		4.70 ± 1.02	35.0 ± 10.2	31.0 (24.6 - 40.2)
85		0.240 ± 0.118	8.00 ± 1.38	0.677 (0.630 - 0.728)
86		0.187 ± 0.017	13.0 ± 3.0	9.20 (8.54 - 10.01)
87		0.356 ± 0.032	1.09 ± 0.22	0.989 (0.921 - 1.062)

Table 2. Continued

Compound	R	IC ₅₀ BRAF (μM) ± SEM	IC ₅₀ pERK (μM) ± SEM	GI ₅₀ SRB (μM) (95% CI)
“Reversed amide”: X = CONH				
88		0.590 ± 0.112	2.05 ± 0.30	3.47 (3.25 - 3.72)
89		0.500 ± 0.079	14.8 ± 2.0	32.0 (26.7 - 38.1)
“Reduced amide”: X = CH ₂				
67		> 10	> 100	0.740 (0.693 - 0.796)

group, the compound bearing an urea linker is more potent than its parent or reversed amide analogues (**12** versus **17** and **83**), whereas when the same ring is substituted by a *tert*-butyl group, compounds with an amide linker are more active than the corresponding urea-linked compounds (e.g., **48** versus **24**). With a pyrazole derivative C-ring, the reversed amide or urea linkers are almost equipotent (**27** versus **87**).

It is clear that the meta substituted middle ring allows a wider range of linkers compared to its para counterpart. Among the linkers explored, amides, sulfonamides, and ureas are active for the meta substitution, while for the para-substituted compounds only the urea group is tolerated.¹⁴

Substitutions on the B Ring. The SAR of the B ring was also examined to optimize potency, and the results are summarized in Table 3. Rings A (2,3-dihydroimidazo[4,5]pyridin-2-one) and C (3-trifluoromethoxyphenyl) and the BC amide linker were kept constant. The compound of reference for this study is **39**, with no substituent on B ring. The insertion of a methyl group in position 2, 4, or 6 (compounds **70**, **68**, or **69**, respectively) has a detrimental effect on activity, leading to inactive compounds. Chlorine has been introduced in various positions of the B ring (compounds **71**–**73**). The 2,4-substitution is tolerated (**72**) but does not improve the biological activity with respect to the parent compound. In contrast, the insertion of a methoxy group in position 5 improves the SRB activity but is detrimental to pERK activity. The incorporation of one or several atoms of fluorine on the B ring (**76**–**78**) leads to compounds with good activities against ^{V600E}BRAF and slightly improved activities in the cell-based assays. Overall, these results are consistent with the meta substituents buttressing the BPI pocket of the BRAF protein, as depicted in Figure 2.

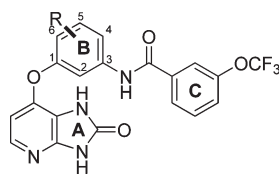
Kinase Selectivity. We anticipated that the change in the geometry of the central middle ring would influence the selectivity profile of the meta-substituted inhibitors. To evaluate this change in selectivity, we submitted compounds **27**, **78**, and **87** (with a ^{V600E}BRAF IC₅₀ of 89, 7, and 356 nM, respectively) to the MRC National Centre for Protein Kinase Profiling²⁰ for the assessment of their activity at a single concentration of 1 μM in a panel of 69–77 protein

kinases. The compounds were chosen in order to provide the widest possible structural diversity, with **27** presenting a urea BC linker and a pyrazole C ring, **78** an amide linker and a phenyl C ring, and **87** a reversed amide linker and a pyrazole C ring. We show here that the three compounds display an improvement in the selectivity profile with respect to the previously reported para series,¹⁵ with no significant inhibition reported against most of the kinases of the panel (see Figure 5). SRC, LCK, and p38α and p38β (MAP) kinases are common hits with all the compounds, with the exception of **87** (see Figure 5). This is unsurprising, as the same three proteins have been shown to be sensitive to type II ligands that, like **78**, elaborate into the BPI pocket.^{15,21–23}

Interestingly, the selectivity of the meta compounds is further enhanced when the urea linker is replaced by an amide. Compound **87**, bearing a phenylpyrazole C-ring and a reverse amide linker, appears remarkably selective within the kinase panel, inhibiting only p38α and, to a lesser extent, p38β and JNK. In addition, compound **78** shows remarkable selectivity in view of its potency (^{V600E}BRAF IC₅₀ of 7 nM), as it inhibits only SRC, LCK, and p38α and p38β.

To assess further the selectivity profile of the series, the IC₅₀ of the same three compounds was assessed by Invitrogen against a focused panel of 16 protein kinases. The results are summarized in Table 4. It is notable that all the compounds assessed are more active on ^{V600E}BRAF than on ^{WT}BRAF, ranging from a 3-fold selectivity for **87** to 30-fold selectivity for **27**. Among the kinases tested in this panel, the compounds show activity only toward the BRAF isoform CRAF and to a partial extent toward KDR and RET.

Cellular Selectivity. In order to provide evidence for the specificity of the compounds for BRAF-driven cell proliferation, the SRB GI₅₀ for the BRAF wild-type WM1361 melanoma cell line was determined for compounds **27** and **87** and compared to the SRB GI₅₀ on the mutant BRAF melanoma cell line WM266.4. The results are shown in Figure 6, along with the SRB GI₅₀ of the multikinase inhibitor sorafenib on the same cell lines. While for sorafenib the activity is independent of BRAF status, our inhibitors are up to 53-fold selective for the mutant BRAF WM266.4 cell line. This selectivity strongly supports our proposed

Table 3. Optimization of B Ring

Compound	B ring	IC ₅₀ BRAF (μM)	IC ₅₀ pERK (μM)	GI ₅₀ SRB (μM)
39		0.014 ± 0.001	7.56 ± 4.93	1.000 (0.916 - 1.092)
68		> 10	> 100	n.d
69		> 10	> 100	38.0 (33.8 - 42.6)
70		> 10	> 100	38.9 (35.5 - 42.5)
71		0.240 ± 0.070	> 100	35.0 (32.5 - 38.0)
72		0.770 ± 0.210	> 100	1.20 (1.09 - 1.28)
73		0.033 ± 0.010	11.3 ± 4.7	1.90 (1.63 - 2.29)
74		0.340 ± 0.120	> 100	4.10 (3.81 - 4.45)
75		0.064 ± 0.031	16.6	0.680 (0.600 - 0.778)
76		0.033 ± 0.010	16.0 ± 2.1	2.40 (2.30 - 2.67)
77		0.010 ± 0.001	6.90 ± 1.56	4.60 (4.36 - 4.84)
78		0.007 ± 0.001	4.05 ± 0.53	4.70 (4.52 - 4.89)

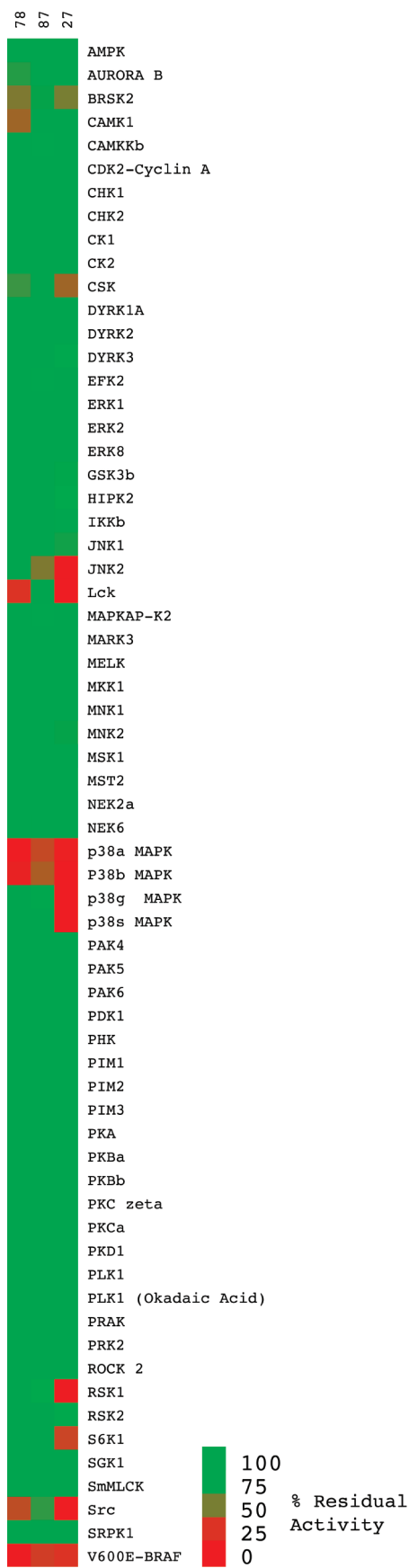


Figure 5. Kinase selectivity of compounds **27**, **78**, and **87** tested against a panel of 69 kinases at the MRC National Centre for Protein Kinase Profiling. The color bar represents the percent activity relative to the control.

Table 4. IC₅₀ (μM) of Selected Compounds **27**, **78**, and **87** toward a Panel of Protein Kinases

kinase	27	78	87
V600E-BRAF	0.089	0.007	0.356
WT-BRAF	3.140	0.042	1.090
FGFR1	> 10	> 10	4.250
FLT1 (VEGFR1)	1.530	4.840	4.160
KDR (VEGFR2)	0.196	0.200	1.370
KIT	1.340	0.216	0.883
LCK	0.584	5.020	> 10
COT	> 10	> 10	> 10
p38γ	1.810	> 10	> 10
p38α	0.152	0.608	1.500
MET	> 10	> 10	> 10
PDGFRα	1.840	2.170	9.710
PDGFRβ	1.550	2.390	7.490
CRAF (DD)	0.198	0.003	0.126
RET	0.698	0.237	0.202

mechanism of action of this series through the inhibition of oncogenic BRAF.

In Vitro Potency and Cellular Activity. It is noted that in the case of some compounds, e.g., **78**, there is a large differential between the potency for V^{600E}BRAF in vitro kinase inhibition and the cellular assays. This is likely to be due to a number of factors such as greater ATP concentration in cells, the extent of compound uptake by the cells, and lipophilicity.

Importantly, our selected compounds show a close correlation between the inhibition of both ERK phosphorylation and cell proliferation in a BRAF mutant cell line. These cells are absolutely dependent upon mutant BRAF-mediated activation of the ERK MAPK pathway, and therefore, loss of ERK phosphorylation is tightly associated with loss of BRAF kinase activity and decreased proliferation.

Conclusion

We have synthesized a novel series of type II BRAF inhibitors in which the aromatic middle ring connects to the hinge binder and the allosteric pocket binder in a 1,3-substitution pattern. This new scaffold shows potent activity in a V^{600E}BRAF assay and allows the use of a wider range of linkers and terminal C rings as salt bridge and allosteric pocket binders, respectively. The introduction of one or more atoms of fluorine on the central B ring achieves low-nanomolar potencies on the V^{600E}BRAF enzyme assay and submicromolar potencies for several compounds. An important advantage of this series of BRAF inhibitors is the improved selectivity against other kinases and improved cellular selectivity compared to the parent para series, as shown by the assessment of selected inhibitors from this series on two panels of protein kinases.

Experimental Section

All starting materials, reagents, and solvents for reactions were reagent grade and used as purchased. Chromatography solvents were HPLC grade and were used without further purification. Reactions were monitored by thin layer chromatography (TLC) analysis using Merck silica gel 60 F-254 thin layer plates. LCMS analyses were performed on a Micromass LCT/Water's Alliance 2795 HPLC system with a Discovery 5 μm, C18, 50 mm × 4.6 mm i.d. column from Supelco at a temperature of 22 °C using the following solvent systems. Solvent A: methanol. Solvent B: 0.1% formic acid in water at a flow rate of 1 mL/min. Gradient starting with 10% A/90% B from 0 to 0.5 min and then 10% A/90% B to

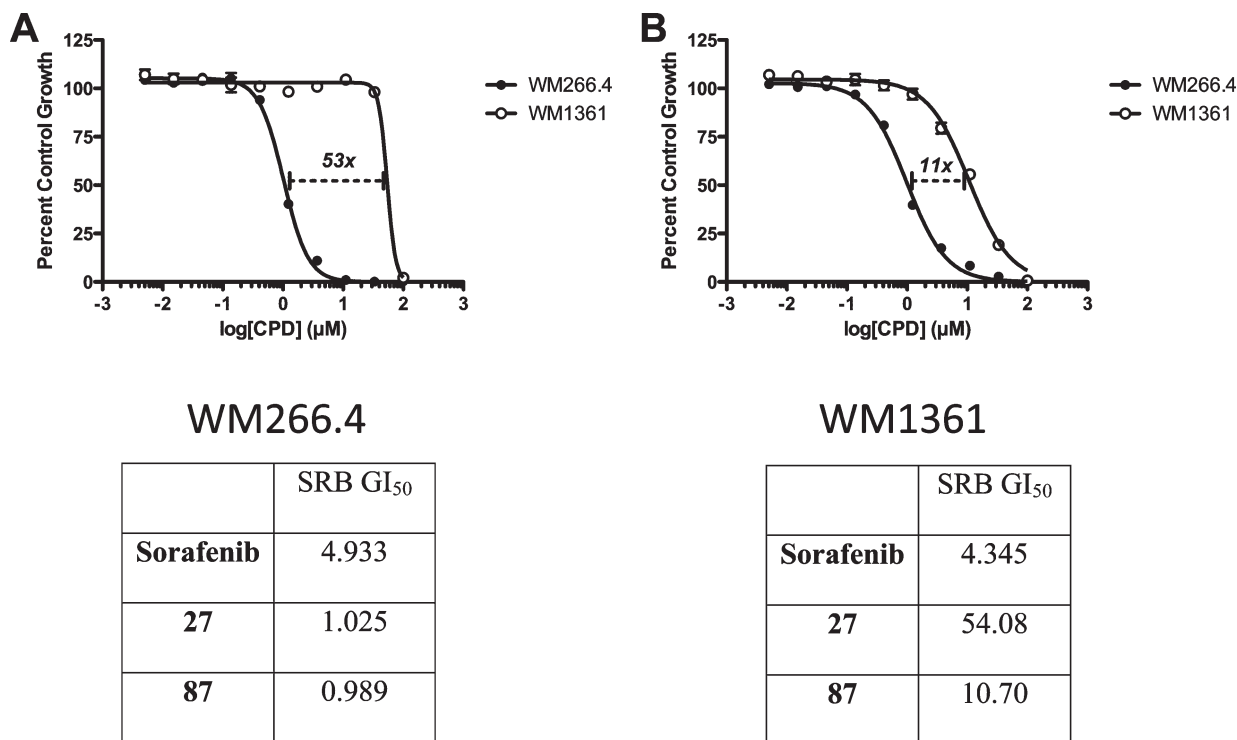


Figure 6. Growth inhibition of WM266.4 (BRAF mutant) and WM1361 (NRAS mutant) melanoma cell lines following a 5-day exposure to **27** (A) or **87** (B) and analysis by SRB assay.

90% A/10% B from 0.5 to 6.5 min and continuing at 90% A/10% B up to 10 min. From 10 to 10.5 min the gradient reverted back to 10% A/90% where the concentrations remained until 12 min. UV detection was at 254 nm, and ionization was positive or negative ion electrospray. Molecular weight scan range is 50–1000. Samples were supplied as 1 mg/mL in DMSO or methanol with 3 μ L injected on a partial loop fill. NMR spectra were recorded in DMSO-*d*₆ on a Bruker DPX 250 operating at 250.13 MHz or on a Bruker advance 500 operating at 500.26 MHz. The signal of the deuterated solvent was used as internal reference; the chemical shifts are expressed in ppm (δ). Coupling constants (*J*) are given in Hz. HRMS analyses were performed on Agilent 6210 time of flight mass spectrometer with an Agilent 1200 series HPLC system. The internal references were caffeine ([M + H]⁺ 195.087 652), reserpine ([M + H]⁺ 609.280 657), and (1*H*,1*H*,3*H*-tetrafluoropentoxo)phosphazene ([M + H]⁺ 922.009 798). Mobile phase consisted of 0.1% formic acid in doubly distilled deionized water (solvent A) and HPLC-grade methanol (solvent B) with all runs executed at 1.0 mL/min flow rate. For condition A, the column Restek Ultra Aqueous 3 μ m C18 (30 mm \times 4.6 mm i.d.) was used with a gradient starting at 90:10 (A/B) from 0.0 to 0.2 min, then 90:10 to 10:90 from 0.2 to 4.0 min, and continuing at 10:90 from 4.0 to 9.25 min before reverting back to 90:10 at 10 min. The purity of the final compounds was determined by HPLC as described above and is 95% or higher unless specified otherwise.

Biological Assays. ^{V600E}**BRAF Kinase Assay and SRB IC₅₀ for BRAF Inhibitors.** These assays have been described by Niculescu-Duvaz et al.¹⁴

pERK Kinase Assay. This assay has been described by Ménard et al.¹⁵

Docking. Inhibitors **12** and **12a** were docked on BRAF (PDB code UWH) using GOLD, version 3.1.1.²⁴ In order to prepare the receptor for docking, the crystal structure was protonated using the Protonate3D tool of MOE, and the ligand and water molecules were then removed. The active site was defined using a radius of 10 Å from the backbone oxygen atom of Asp594 of the ATP binding pocket. Partial charges of the ligands were derived using the Charge-2 CORINA 3D package in TSAR 3.3 and their

geometries optimized using the COSMIC module of TSAR. The calculations were terminated if the energy difference or the energy gradient were smaller than 1×10^{-5} . Ten docking solutions were generated per docking run with GOLD, and the best three were stored for analysis.

1-(4-Chloro-3-(trifluoromethyl)phenyl)-3-(3-(2-oxo-2,3-dihydro-1*H*-imidazo[4,5-*b*]pyridin-7-yloxy)phenyl)urea (12**).** **Method A.** A mixture of 4-chloro-3-(trifluoromethyl)phenyl isocyanate (33 mg, 0.16 mmol) and 7-(3-aminophenoxy)-1*H*-imidazo[4,5-*b*]pyridin-2(3*H*)-one **8a** (30 mg, 0.13 mmol) in anhydrous THF (1.5 mL) was stirred at room temperature for 14 h. Next, the solvent was evaporated and the solid residue was washed with Et₂O to afford **12** as an off-white solid (33 mg, 55%). ¹H NMR δ : 6.45 (d, 1H, H_{Py,5}, *J* = 5.8), 6.78 (d, 1H, H_{arom}, *J* = 8.2), 7.25 (d, 1H, H_{arom}, *J* = 7.9), 7.34–7.39 (m, 2H, H_{arom}), 7.55–7.67 (m, 2H, H_{arom}), 7.79 (d, 1H, H_{Py,6}, *J* = 5.8), 8.06 (s, 1H, H_{arom}), 9.14 (s, 1H, NH_{urea}), 9.29 (s, 1H, NH_{urea}), 11.23 (s, 1H, NH), 11.42 (s, 1H, NH). LC–MS: *m/z* 464 (M + H, 100). HRMS: *m/z* calcd for C₂₀H₁₄ClF₃N₅O₃ ([M + H]⁺), 464.0737; found, 464.0727.

4-Chloro-*N*-(3-(2-oxo-2,3-dihydro-1*H*-imidazo[4,5-*b*]pyridin-7-yloxy)phenyl)-3-(trifluoromethyl)benzenesulfonamide (13**).** **Method B.** 7-(3-Aminophenoxy)-1*H*-imidazo[4,5-*b*]pyridine-2(3*H*)-one **8a** (30 mg, 0.13 mmol) was suspended in dry pyridine (3 mL), and 4-chloro-3-(trifluoromethyl)benzene-1-sulfonyl chloride (44.4 mg, 0.16 mmol) in pyridine (2 mL) was added. The resulting solution was stirred at room temperature for 20 h, and subsequently the solvent was removed in vacuo. The obtained residue was dissolved in acetone (4 mL), and upon addition of water a solid precipitated. This solid was collected, washed with water (2 \times 2 mL) and Et₂O (2 \times 2 mL), and dried under vacuum. **13** was obtained as an off-white solid (38 mg, 60%). ¹H NMR δ : 6.23 (d, 1H, H_{Py,5}, *J* = 5.7), 6.76–6.98 (m, 3H, H_{arom}), 7.35 (m, 1H, H_{arom}), 7.73 (m, 1H, H_{arom}), 7.94–7.96 (m, 2H, H_{arom}), 8.05 (d, 1H, H_{Py,6}, *J* = 5.7) 10.62 (s, 1H, NHSO₂), 11.13 (s, 1H, NH), 11.40 (s, 1H, NH). LC–MS: *m/z* 485 (M + H, 100). HRMS: *m/z* calcd for C₁₉H₁₃ClF₃N₄O₄S ([M + H]⁺), 485.0298; found, 485.0297.

***N*-(2,3,4-Trifluoro-5-(2-oxo-2,3-dihydro-1*H*-imidazo[4,5-*b*]pyridin-7-yloxy)phenyl)-3-(trifluoromethoxy)benzamide (78).**

Method C. *N*-(5-(2,3-Diaminopyridin-4-yloxy)-2,3,4-trifluorophenyl)-3-(trifluoromethoxy)benzamide **111** (90 mg, 0.20 mmol) and triethylamine (35 μ L, 0.25 mmol) were mixed in dry THF (7.7 mL), and 3-(trifluoromethoxy)benzoyl chloride (57 mg, 0.25 mmol) was added. This mixture was heated to reflux for 20 h, and subsequently the solvent was removed in vacuo. The obtained residue was dissolved in acetone (3 mL), and upon addition of water a solid precipitated. This solid was collected, washed with water (2 \times 3 mL) and Et₂O (2 \times 3 mL), and dried to afford the title compound **78** (39 mg, 40%). ¹H NMR δ : 6.65 (d, 1H, H_{Py,5}, *J* = 6.0), 7.32 (t, 1H, H_{arom}, *J* = 6.5), 7.63 (d, 1H, H_{arom}, *J* = 8.0), 7.68 (t, 1H, H_{arom}, *J* = 8.0), 7.84 (d, 1H, H_{Py,6}, *J* = 6.0), 7.88 (s, 1H, H_{arom}), 7.98 (d, 1H, H_{arom}, *J* = 8.0), 10.52 (s, 1H, NH_{amide}), 11.26 (s, 1H, NH_{Im3}), 11.47 (s, 1H, NH_{Im2}). LC–MS: *m/z* 485 (M + H, 100). HRMS: *m/z* calcd for C₂₀H₁₁F₆N₄O₄ ([M + H]⁺), 485.06790; found 485.06708.

***N*-(3-(2-Oxo-2,3-dihydro-1*H*-imidazo[4,5-*b*]pyridin-7-yloxy)-phenyl)-2-(3-trifluoromethylphenyl)acetamide (31).** **31** was synthesized following method C with 2-(3-trifluoromethylphenyl)acetyl chloride (44 μ L, 0.25 mmol). Yield: 30 mg, 33.3%.

***N*-(3-(2-Oxo-2,3-dihydro-1*H*-imidazo[4,5-*b*]pyridin-7-yloxy)-phenyl)-3-phenyl propanamide (36).** **36** was synthesized following method C with 3-phenylpropanoyl chloride (37 μ L, 0.25 mmol). Yield: 15 mg, 19%.

7-(3-(3-(Trifluoromethoxy)benzylamino)phenoxy)-1*H*-imidazo[4,5-*b*]pyridin-2(3*H*)-one (67). 7-(3-Aminophenoxy)-1*H*-imidazo[4,5-*b*]pyridin-2(3*H*)-one **8a** (80 mg, 0.330 mmol) was stirred in dry EtOH (1.5 mL) with 3-(trifluoromethoxy)benzaldehyde (140 μ L, 0.99 mmol) under argon for 1 h. Then sodium triacetoxyborohydride (210 mg, 0.99 mmol) was added followed by glacial acetic acid (0.35 mL). This mixture was stirred at room temperature overnight, and the solvent was removed in vacuo. The obtained residue was retaken in EtOAc, washed with water and a saturated solution of NaHCO₃, dried over MgSO₄, and concentrated under vacuum. The obtained residue was purified by chromatography using a SCX-2 column (eluent MeOH and a solution of NH₃ in MeOH), and **67** was obtained as a dark-pink solid (95 mg, 69%). ¹H NMR δ : 4.32 (d, 2H, CH₂, *J* = 6.1), 6.27–6.31 (m, 3H, H_{arom}), 6.48 (dd, 1H, H_{arom}, *J* = 8.2, *J* = 1.4), 6.58 (t, 1H, NH_{amine}, *J* = 6.1), 7.10 (t, 1H, H_{arom}, *J* = 8.1), 7.21 (d, 1H, H_{arom}, *J* = 7.8), 7.29 (s, 1H, H_{arom}), 7.36 (d, 1H, H_{arom}, *J* = 7.7), 7.45 (t, 1H, H_{arom}, *J* = 7.9), 7.70 (d, 1H, H_{arom}, *J* = 5.9), 11.08 (s, 1H, NH_{Im}), 11.29 (s, 1H, NH_{Im}). LC–MS: *m/z* 417 (M + H, 100). HRMS: *m/z* calcd for C₂₀H₁₅F₃N₄O₃ ([M + H]⁺), 417.1169; found, 417.1169.

***N*-(4-Chloro-3-(trifluoromethyl)phenyl)-3-(2-oxo-2,3-dihydro-1*H*-imidazo[4,5-*b*]pyridin-7-yloxy)benzamide (83).** **Method D.** A solution of AlMe₃ (solution in 2 M toluene, 450 μ L, 0.890 mmol) was added dropwise to a cooled (0 °C) solution of 4-chloro-3-(trifluoromethyl)aniline (174 mg, 0.890 mmol) in THF (3.5 mL). When the addition was complete, the mixture was allowed to warm to room temperature and the stirring was continued for 30 min. Then **81** (101 mg, 0.356 mmol) was added and the mixture was heated under reflux for 19 h. The mixture was cooled to room temperature and carefully quenched with 5% aqueous HCl (1.5 mL). After evaporation of solvent, the residue was retaken in CH₂Cl₂, washed with saturated solution of NaHCO₃ and then with brine, dried over MgSO₄, and evaporated under vacuum. The obtained residue was chromatographed (eluent EtOAc), and **83** was obtained as a slightly yellow solid (48 mg, 30%).

Acknowledgment. This work is supported by Cancer Research UK (grants C309/A2187 and C107/A10433), the Wellcome Trust, the Institute of Cancer Research, and the Isle of Mann Anti-Cancer Association. We acknowledge NHS funding to the NIHR Biomedical Research Centre. Professors Paul Workman and Julian Blagg are acknowledged for their

strong support and helpful reading of the manuscript. Meirion Richards, Dr. Maggie Liu, and Dr. Amin Mirza are thanked for providing technical assistance.

Supporting Information Available: Experimental details of the synthesis of compounds **14–30**, **32–35**, **37–66**, **68–77**, **79–82**, and **84–89** and intermediates; analytical characterization of all compounds. This material is available free of charge via the Internet at <http://pubs.acs.org>.

References

- (1) Wellbrock, C.; Ogilvie, L.; Hedley, D.; Karasarides, M.; Martin, J.; Niculescu-Duvaz, D.; Springer, C. J.; Marais, R. V599EB-RAF is an oncogene in melanocytes. *Cancer Res.* **2004**, *64*, 2338–2342.
- (2) Wellbrock, C.; Karasarides, M.; Marais, R. The RAF proteins take centre stage. *Nat. Rev. Mol. Cell Biol.* **2004**, *5*, 875–885.
- (3) Davies, H.; Bignell, G. R.; Cox, C.; Stephens, P.; Edkins, S.; Clegg, S.; Teague, J.; Woffendin, H.; Garnett, M. J.; Bottomley, W.; Davis, N.; Dicks, E.; Ewing, R.; Floyd, Y.; Gray, K.; Hall, S.; Hawes, R.; Hughes, J.; Kosmidou, V.; Menzies, A.; Mould, C.; Parker, A.; Stevens, C.; Watt, S.; Hooper, S.; Wilson, R.; Jayatilake, H.; Gusterson, B. A.; Cooper, C.; Shipley, J.; Hargrave, D.; Pritchard-Jones, K.; Maitland, N.; Chenevix-Trench, G.; Riggins, G. J.; Bigner, D. D.; Palmieri, G.; Cossu, A.; Flanagan, A.; Nicholson, A.; Ho, J. W.; Leung, S. Y.; Yuen, S. T.; Weber, B. L.; Seigler, H. F.; Darrow, T. L.; Paterson, H.; Marais, R.; Marshall, C. J.; Wooster, R.; Stratton, M. R.; Futreal, P. A. Mutations of the BRAF gene in human cancer. *Nature* **2002**, *417*, 949–954.
- (4) Wan, P. T.; Garnett, M. J.; Roe, S. M.; Lee, S.; Niculescu-Duvaz, D.; Good, V. M.; Jones, C. M.; Marshall, C. J.; Springer, C. J.; Barford, D.; Marais, R. Mechanism of activation of the RAF-ERK signaling pathway by oncogenic mutations of B-RAF. *Cell* **2004**, *116*, 855–867.
- (5) Gray-Schopfer, V.; Wellbrock, C.; Marais, R. Melanoma biology and new targeted therapy. *Nature* **2007**, *445*, 851–857.
- (6) Hingorani, S. R.; Jacobetz, M. A.; Robertson, G. P.; Herlyn, M.; Tuveson, D. A. Suppression of BRAF(V599E) in human melanoma abrogates transformation. *Cancer Res.* **2003**, *63*, 5198–5202.
- (7) Karasarides, M.; Chiloeches, A.; Hayward, R.; Niculescu-Duvaz, D.; Scanlon, I.; Friedlos, F.; Ogilvie, L.; Hedley, D.; Martin, J.; Marshall, C. J.; Springer, C. J.; Marais, R. B-RAF is a therapeutic target in melanoma. *Oncogene* **2004**, *23*, 6292–6298.
- (8) Roberts, P. J.; Der, C. J. Targeting the Raf-MEK-ERK mitogen-activated protein kinase cascade for the treatment of cancer. *Oncogene* **2007**, *26*, 3291–3310.
- (9) Smith, R. A.; Dumas, J.; Adnane, L.; Wilhelm, S. M. Recent advances in the research and development of RAF kinase inhibitors. *Curr. Top. Med. Chem.* **2006**, *6*, 1071–1089.
- (10) Barker, A. J.; Gibson, K. H.; Grundy, W.; Godfrey, A. A.; Barlow, J. J.; Healy, M. P.; Woodburn, J. R.; Ashton, S. E.; Curry, B. J.; Scarlett, L.; Henthorn, L.; Richards, L. Studies leading to the identification of ZD1839 (IRESSA): an orally active, selective epidermal growth factor receptor tyrosine kinase inhibitor targeted to the treatment of cancer. *Bioorg. Med. Chem. Lett.* **2001**, *11*, 1911–1914.
- (11) Lowinger, T. B.; Riedl, B.; Dumas, J.; Smith, R. A. Design and discovery of small molecules targeting raf-1 kinase. *Curr. Pharm. Des.* **2002**, *8*, 2269–2278.
- (12) Capdeville, R.; Buchdunger, E.; Zimmermann, J.; Matter, A. Glivec (ST1571, imatinib), a rationally developed, targeted anti-cancer drug. *Nat. Rev. Drug Discovery* **2002**, *1*, 493–502.
- (13) Liu, Y.; Gray, N. S. Rational design of inhibitors that bind to inactive kinase conformations. *Nat. Chem. Biol.* **2006**, *2*, 358–364.
- (14) Niculescu-Duvaz, D.; Gaulon, C.; Dijkstra, H. P.; Niculescu-Duvaz, I.; Zambon, A.; Menard, D.; Suijkerbuijk, B. M.; Nourry, A.; Davies, L.; Manne, H.; Friedlos, F.; Ogilvie, L.; Hedley, D.; Whittaker, S.; Kirk, R.; Gill, A.; Taylor, R. D.; Raynaud, F. I.; Moreno-Farre, J.; Marais, R.; Springer, C. J. Pyridoimidazolones as novel potent inhibitors of v-Raf murine sarcoma viral oncogene homologue B1 (BRAF). *J. Med. Chem.* **2009**, *52*, 2255–2264.
- (15) Menard, D.; Niculescu-Duvaz, I.; Dijkstra, H. P.; Niculescu-Duvaz, D.; Suijkerbuijk, B. M.; Zambon, A.; Nourry, A.; Roman, E.; Davies, L.; Manne, H. A.; Friedlos, F.; Kirk, R.; Whittaker, S.; Gill, A.; Taylor, R. D.; Marais, R.; Springer, C. J. Novel potent BRAF inhibitors: toward 1 nM compounds through optimization of the central phenyl ring. *J. Med. Chem.* **2009**, *52*, 3881–3891.

- (16) Liao, J. J. Molecular recognition of protein kinase binding pockets for design of potent and selective kinase inhibitors. *J. Med. Chem.* **2007**, *50*, 409–424.
- (17) Tsai, J.; Lee, J. T.; Wang, W.; Zhang, J.; Cho, H.; Mamo, S.; Bremer, R.; Gillette, S.; Kong, J.; Haass, N. K.; Sproesser, K.; Li, L.; Smalley, K. S.; Fong, D.; Zhu, Y. L.; Marimuthu, A.; Nguyen, H.; Lam, B.; Liu, J.; Cheung, I.; Rice, J.; Suzuki, Y.; Luu, C.; Settachatgul, C.; Shellooe, R.; Cantwell, J.; Kim, S. H.; Schlessinger, J.; Zhang, K. Y.; West, B. L.; Powell, B.; Habets, G.; Zhang, C.; Ibrahim, P. N.; Hirth, P.; Artis, D. R.; Herlyn, M.; Bollag, G. Discovery of a selective inhibitor of oncogenic B-Raf kinase with potent antimelanoma activity. *Proc. Natl. Acad. Sci. U.S.A.* **2008**, *105*, 3041–3046.
- (18) Correa, A.; Tellitu, I.; Dominguez, E.; SanMartin, R. Novel alternative for the N–S bond formation and its application to the synthesis of benzisothiazol-3-ones. *Org. Lett.* **2006**, *8*, 4811–4813.
- (19) Wang, J.; Rosingana, M.; Discordia, R. P.; Soundararajan, N.; Polniaszek, R. Aminolysis of esters or lactones promoted by NaHMDS, a general and efficient method for the preparation of *N*-aryl amides. *Synlett* **2001**, *9*, 1485–1487.
- (20) Davies, S. P.; Reddy, H.; Caivano, M.; Cohen, P. Specificity and mechanism of action of some commonly used protein kinase inhibitors. *Biochem. J.* **2000**, *351*, 95–105.
- (21) Filippakopoulos, P.; Barr, A.; Fedorov, O.; Keates, T.; Soundararajan, M.; Elkins, J.; Salah, E.; Burgess-Brown, N.; Ugochukwu, E.; Pike, A. C. W.; Muniz, J.; Roos, A.; Chaikuad, A.; von Delft, F.; Arrowsmith, C. H.; Edwards, A. M.; Weigelt, J.; Bountra, C.; Knapp, S. Crystal Structure of Human Mitogen Activated Protein Kinase 11 (p38 beta) in Complex with Nilotinib. Structural Genomics Consortium. PDB code: 3GP0 (<http://www.rcsb.org/pdb/home/home.do>), **2009**.
- (22) Seeliger, M. A.; Nagar, B.; Frank, F.; Cao, X.; Henderson, M. N.; Kuriyan, J. c-Src binds to the cancer drug imatinib with an inactive Abl/c-Kit conformation and a distributed thermodynamic penalty. *Structure* **2007**, *15*, 299–311.
- (23) Jacobs, M. D.; Caron, P. R.; Hare, B. J. Classifying protein kinase structures guides use of ligand-selectivity profiles to predict inactive conformations: structure of lck/imatinib complex. *Proteins* **2008**, *70*, 1451–1460.
- (24) Jones, G.; Willett, P.; Glen, R. C.; Leach, A. R.; Taylor, R. Development and validation of a genetic algorithm for flexible docking. *J. Mol. Biol.* **1997**, *267*, 727–748.